Spiral twisting of fiber orientation inside bone lamellae

W. Wagermaier, H. S. Gupta, and A. Gourrier
Department of Biomaterials, Max Planck Institute of Colloids and Interfaces, Potsdam 14424, Germany

M. Burghammer
ESRF, European Synchrotron Radiation Facility, Grenoble 30843, France

P. Roschger
Ludwig Boltzmann Institute of Osteology at the Hanusch Hospital of WGKK and AUVA Trauma Centre Meidling, Vienna 1120, Austria

P. Fratzl[a)]
Department of Biomaterials, Max Planck Institute Colloids and Interfaces, Potsdam 14424, Germany

The secondary osteon — a fundamental building block in compact bone — is a multilayered cylindrical structure of mineralized collagen fibrils arranged around a blood vessel. Functionally, the osteon must be adapted to the *in vivo* mechanical stresses in bone at the level of its microstructure. However, questions remain about the precise mechanism by which this is achieved. By application of scanning x-ray diffraction with a micron-sized synchrotron beam, along with measurements of local mineral crystallographic axis direction, we reconstruct the three-dimensional orientation of the mineralized fibrils within a single osteon lamella (~ 5 μm). We find that the mineralized collagen fibrils spiral around the central axis with varying degrees of tilt, which would — structurally — impart high extensibility to the osteon. As a consequence, strains inside the osteon would have to be taken up by means of shear between the fibrils. © *2006 American Vacuum Society.*
[DOI: 10.1116/1.2178386]

I. INTRODUCTION

Bone is a fibrous composite, consisting of carbonated apatite embedded in an organic collagen framework.[1] The character of lamellar bone, the most abundant type in many mammals, is widely discussed but there is still no full agreement on the detailed structure. It has been proposed that the fiber arrangement is a twisted plywood system or an orthogonal plywood structure.[2] Rho[3] pointed out the necessity of understanding the structural variation at the fibrillar level to model and explain the properties of the material bone. In general, during development of skeletal systems fibers are manipulated into precise directions within the supporting tissues to be best adapted to their mechanical functions.[4] Different approaches have been taken in solving these questions on different length scales, from static structure investigations[5] to *in situ* mechanical testing.[6]

Compact bone, which is found in the cylindrical shells of most long bones in vertebrates, consists of lamellae that are cylindrically wrapped around blood vessels (Haversian systems or secondary osteons). These secondary osteons, whose mechanical properties are crucial to the structural stability of the entire bone, form during bone remodelling.[7] Several authors have shown[8,9] that the orientation of the collagen fibers is a function of external stresses on the bone, and that these variations might enable structures to adapt to and better resist the applied forces. When single osteons are cyclically loaded, synchrotron x-ray diffraction measurements of the (averaged) mineral crystal orientation show that on average, reorientation of the c axis occurs in the direction of applied load parallel to the osteon axis.[10]

Blood vessels, as the main transport system for oxygen, carbon dioxide, and several other elements, require a special protection inside the bone. Therefore the structure of an osteon has to fulfill this function. Ascenzi and co-workers described, via detailed x-ray diffraction experiments, the structural differences between varying isolated osteonal lamellae.[11] Mineral particles appeared differently oriented in specimens that appear dark and bright under polarized light microscopy. In general — and specifically concerning mechanical isolation — it is difficult to define "one single lamella." To deduce mechanical implications for the osteon, the structure of the lamellae has to be investigated at the fibrillar level.[1]

To attain this goal, a combination of texture analysis and scanning x-ray diffraction is an appropriate strategy. Texture analysis can be used as a quantitative method for determining the crystal orientation in bone[10,12,13] Scanning x-ray experiments with a micrometer sized beam using high brilliance synchrotron radiation[14] enable the measurement of the local mineral orientation of entire osteons. Clearly, only the combination of: (a) a beamsize comparable to or smaller to the size of single lamellae; (b) a sample thickness of the same order of magnitude as the beam diameter (for transmission x-ray measurements); (c) stepwise rotation of the sample for local texture measurements; and (d) alignment of the beam position relative to the fiber orientation in the tissue makes it possible to resolve the local crystallite orientation quantitatively. In this article we present investigations com-
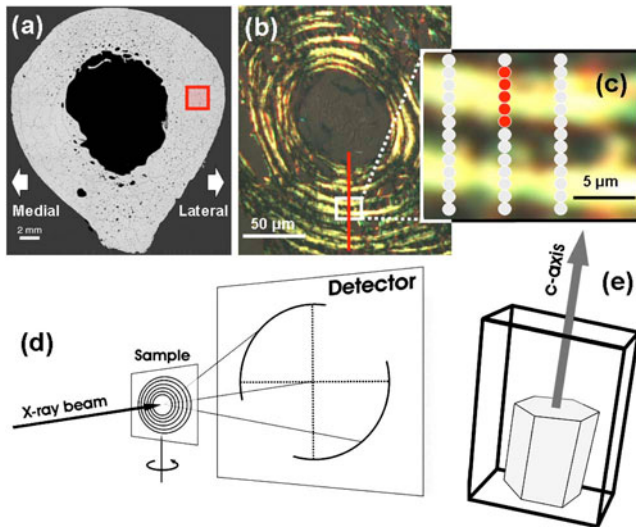

[a)]Electronic mail: fratzl@mpikg.mpg.de

FIG. 1. (a) Cross section of the femoral midshaft. The red square shows the region from where samples originate. (b) Thin section of the human bone observed in transmission with a polarizing light microscope: osteon where brightness of lamellae changes alternately. (c) High magnification zoom shows three alternating lamellae. The red dots indicate the x-ray beam size (1 μm). (d) Schematic of the experimental setup showing the sample rotation, x-ray beam and detector pattern. (e) Schematic of a mineral platelet with a hexagonal unit cell (not drawn to scale) and definition of the crystallographic c axis.

bining these requirements in a scanning texture analysis on several osteons, using a 1 μm synchrotron beam. Quantitative results on mineral crystallite orientation as a function of position on the osteon are shown, with intralamellar resolution.

II. MATERIALS AND METHODS

The bone type used for this investigation was the femoral midshaft from a healthy human female [Fig. 1(a)]. Our investigations are based on circular osteons from the lateral region of the midshaft shell where lamellae appear in polarized light microscopy alternating as dark and bright regions.

A $2 \times 2 \times 10$ mm^3 stick was cut out of the bone using a low speed diamond saw (Buehler Isomet, Lake Bluff Illinois, U.S.). The undecalcified specimens were fixed in ethanol/formalin solution 70:30 v/v and after dehydrating they were embedded in polymethylmetacrylate.[15] With a microtome (Leica SM2500E, Leica Microsystems, Bensheim, Germany) thin sections with a thickness of about 3–4 μm were cut from this block. To check the influence of microtoming on the internal structure of these thin sheets, thicker platelets (50 μm) from the same stick were cut using a diamond inner-hole saw (Leica SP1600, Leica Microsystems, Bensheim, Germany).

Scanning small angle x-ray scattering (SAXS) and wide-angle x-ray diffraction (WAXD) are effective methods for position resolved investigations of bone sections.[16] Thin samples can be scanned with a step-size in the band of the beam size, acquiring two-dimensional SAXS or WAXD patterns at every point. To resolve the lamellae as they appear in polarized light microscopy with a thickness of 5–7 μm an

x-ray beam significantly smaller than the thickness is required, in order to avoid signal irregularities due to overlapping sample volumes at adjacent scan points. Therefore we choose for our investigations a synchrotron x-ray beam with a diameter of 1 μm.

The experiments were performed at the microfocus beamline of the European Synchrotron Radiation Facility (ESRF), Grenoble. The ID13 beamline is characterized by a 18 mm period in-vacuum undulator optimized for 13 keV and the optical setup for a (sub)micrometer beam (variable in a region from 0.5 to 5 μm) is defined by a Kirkpatrick–Baez mirror.[17] The radiation wavelength was 0.9755 Å and a 16 bit readout MARCCD (Mar Inc., U.S.) detector with an x-ray converter screen of 130 mm diameter and 2048×2048 pixels with a pixel size of 64.45×64.45 μm^2 was used for recording the diffraction patterns. For faster readout, data were recorded in binning mode with 512×512 pixels. In the scanning setup [Fig. 1(d)] the samples were fixed on glass capillaries which were attached to a goniometer head. The beam was positioned accurately on a specific point on the sample by using a high resolution microscope. From this point a reproducible scanning grid was defined on the sample and for every single grid point a diffraction pattern was collected. By choosing an appropriate sample to detector distance (130 mm in this case) we obtained diffraction frames in which the SAXS signal and the WAXD (002) reflections from the mineral apatite (along the c axis of hexagonal cubic crystal structure) axis were visible.

Apatite has a hexagonal cubic structure.[18] Heidelbach and co-workers.[19,20] showed that for a full quantitative texture investigation a crystallite orientation distribution analysis is required, with several different diffraction peaks measured simultaneously. However, the aim of our experiment was to give quantitative information about the orientation of the crystallographic c axis of the mineral particles only. The c axis of the mineral particles is aligned first with the long dimension of the mineral platelets [Fig. 1(e)] which in turn is parallel to the collagen fibril direction.[21,22] Therefore we measured the orientation of the (002) pole for individual line scans over several osteons. A line scan runs along the radius of the osteon from the center of the blood vessel into the surrounding cortical bone. Along this line scan at every 1 μm step orientation information is acquired by rotating the sample in steps of 5° from +45° to −45°. For every rotating step a diffraction image is obtained, resulting in 19 individual images which are merged together to give the orientation distribution at one measuring point. To minimize the position correction for every rotation angle we performed the line scans in the vertical direction: one along the rotation axis of the osteon and two more in a relative horizontal distance of ±5 μm to it.

The diffraction images were processed with the software Fit2D.[23] Every image was corrected for transmission, and the intensity distribution with no sample in the beam was subtracted. Due to scattering from the mineral, a subtraction of the diffuse background is necessary to obtain the correct azimuthal intensity profiles, which are used for further data pro-
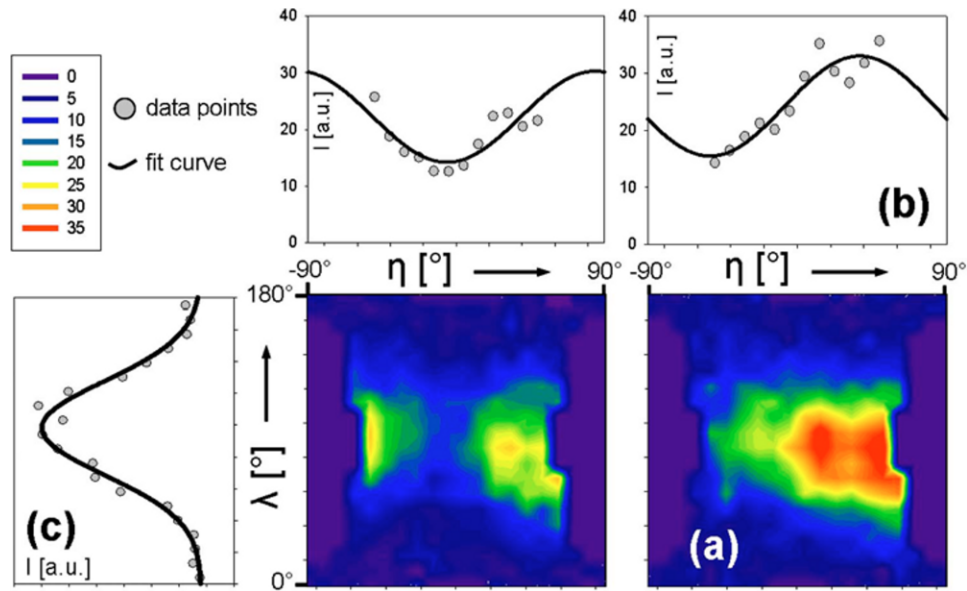
FIG. 2. Two-dimensional stereographic plots and the corresponding line profiles. The color code indicates the intensity of the 002 pole (arbitrary units). Vertical λ profiles are fitted with gaussians, horizontal η profiles with a cosine fit (fixed period of π).

cessing. For a given crystallographic axis the intensity variations of the Debye–Scherrer rings at different rotation angles of the sample are, within a constant scaling factor, traces of the orientation distribution of the axis on a unit sphere in real space. To represent this distribution in two dimensions, a standard stereographic projection is made from the unit sphere to the unit disk in plane.[13] Hence, by using a set of latitude(λ)/longitude(η) coordinates to represent any point in the unit disk, the intensity distribution can be coordinate transformed from spherical polar coordinates to a rectangular grid (latitude/longitude coordinates). We show examples of the resulting two-dimensional (2D) intensity distributions in Fig. 2(a). As a final step in data reduction, we integrated the intensity in the η and λ coordinates, leading to one-dimensional profiles $I(\eta)$ and $I(\lambda)$ as seen in Figs. 2(b) and 2(c). A Gaussian function was used to fit $I(\lambda)$, and for $I(\eta)$, keeping in mind an observed periodic variation, the function $f(\eta) = y0 + a \cdot \cos(2 \cdot \eta + 2 \cdot c)$ was used.

III. RESULTS

In Figs. 1(b) and 1(c) we can see a typical polarized light microscopy image of one of the investigated osteons. The consecutive lamellae show different brightness, alternating from "dark" to "bright," as well documented in the literature.[11] Both sheets (the microtomed 3 μm and the cut 50 μm control sheet) were characterized by polarized light. The osteons of both sheets showed the same principal pattern (alternation of "dark" and "bright" lamellae). The optical effect appears due to birefringence originating from both collagen and the mineral particles. This demonstrates that the orientation of the carbonated apatite particles and the collagen is not influenced by the cutting process with the microtome.

In Fig. 2(a) (vertical) λ profile is shown, which is found to be typical for all measuring points. Since the intensity values are all concentrated within an average full width at half maximum of $50°(\pm25°)$ we conclude that the main variation of the orientation occurs in the horizontal η direction, which also can be clearly seen in all the 2D λ/η plots (Fig. 2). In terms of the osteonal lamellar structure this means the orientation of the c axis of the mineral platelets changes mostly within the plane of a lamella. This can be quantified by analyzing the horizontal η profiles.

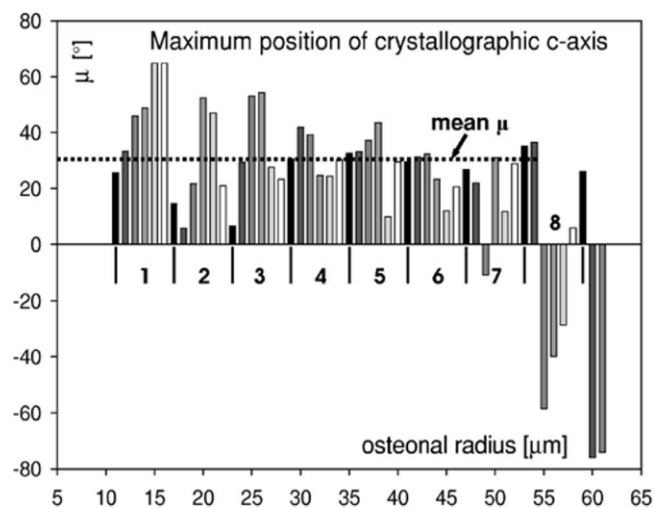Figure 3 shows the maximum position (longitudinal angle

FIG. 3. Value of the individual bars indicate the position of the crystallographic c axis of the carbonated apatite mineral crystals. The angle changes from about 10° to 60° relative to the long axis of the osteon with a periodicity of 5−7 μm. The lamellae at 55−57 μm show a different orientation than the others. From 60 μm upward (last two bars in the graph) the values correspond to interstitial bone.

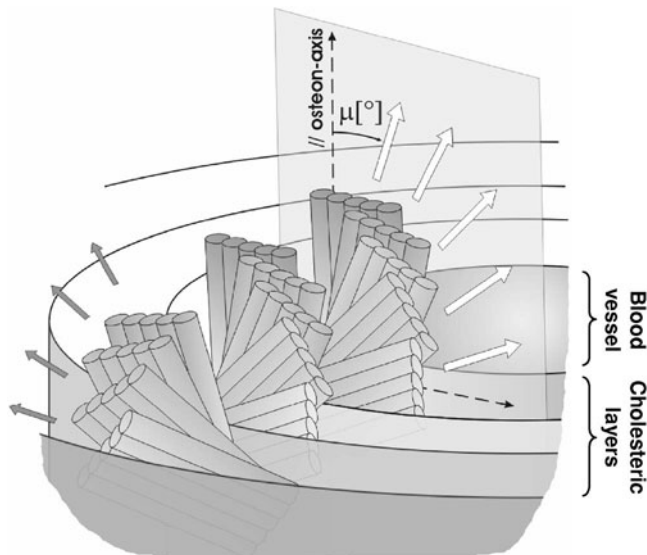FIG. 4. Model of fibrillar orientation relative to the osteon axis. The orientation of the fibrils changes with a periodicity of $5-7$ μm, which corresponds to one single dark or bright lamellae in the polarized light microscopy image. Only the fibrils of the outermost lamella show a different chirality in orientation.

η) of the (002) pole occurrence as a function of the position on the osteon. A step from one bar to the next corresponds to a step size of 1 μm along the measured radial line scan starting in the center of the circular osteon and going vertically down, as per Fig. 2(a). It can be seen that the orientation of the (002) pole changes periodically in an interval of about $5-7$ μm, corresponding to the thickness of the individual lamellae as seen in polarized light microscopy. The maximum position (angle μ) varies from about 10° to 60° relative to the osteon axis in the first innermost lamellae. The difference between the maximum and minimum values decreases as the distance from the osteon center increases. All poles are oriented only within one quadrant $(0°-90°)$ relative to the $(0°)$ axis of the osteon with an average of $\mu \approx 30°$. This indicates a three-dimensional (3D) spiral (helicoidal) arrangement for the fibrils around the blood vessel. Only the outermost lamella shows a different chirality and the fibrils spiral around the vascular channel with the opposite orientation.

All probed osteons from the lateral region of the femoral midshaft [Fig. 1(a)], which were all circular and showed alternating bright and dark regions in polarized light microscopy, delivered similar results and confirmed the unidirectionality of fibrils over most lamellae and the orientation oscillation on a micrometer length scale. The different chirality of the outermost lamella as found in the presented osteon has to be investigated and potentially proved on a higher number of samples.

IV. DISCUSSION

Our investigations address the question of the spatial orientation of the mineral particles within osteonal human bone. With quantitative texture analysis using a synchrotron x-ray

beam we are able to show the mineral crystallite orientation as a function of position on the osteon with a resolution of 1 μm. Figure 4 shows our results qualitatively in a model of fiber orientation within cholesteric layers relative to the osteon long axis. Since the orientation of the fibrils differs only in a range from 0° to 90° we deduce a three-dimensional spiral (helicoidal) appearance of the fibrils, which are wound around the blood vessel within coaxial cylinders. The orientation angle μ of the fibrils relative to the osteon axis in successive cholesteric layers (spacing of 1 μm) changes in a regular sequence of about $5°-25°$, and just at about every sixth cylinder there is a jump in the angle μ of more than $-30°$. The sense of the helical winding is right-handed — similar to wood cells[24] — and the chirality is the same for all lamellae except for the outermost one.

Neville[4] describes naturally occurring Helicoids as cylindrical multidirectional plywoods, with changes in orientation angles from 10° and 20° between neighboring layers. Helicoidal arrangements of fibers are found in several biological tissues, such as insect cuticle[4] and plant cell walls.[25] In wood, variations in the microfibril angle allow a tuning of both stiffness and extensibility of the wood cell and enable the material to adapt to mechanical loading.[26] The microfibril angle has an evident influence on the extensibility of the cell wall. Small microfibril angles provide maximum stiffness of the cell wall, whereas large angles result in maximum extensibility.[27] Giraud-Guille,[2,28] Besseau and Cowin[29] describe (cylindrical) twisted plywood structures of biological tissues analogous to cholesteric liquid crystal flows frozen in time. One of the future prospects given in their studies is to investigate the behavior of stabilized biological mesophases in response to mechanical forces. Helicoidal structures have certain advantages in resisting mechanical loads compared to orthogonal plywood structures since the twisted orientation enables a higher extensibility in tension and compression.

In this context it seems biophysically reasonable that a three-dimensional spiraling of fibrils appears in osteonal bone too. One of the advantages of such a helicoidal plywood structure and its mechanical flexibility would be the protection of the blood vessels against failure of the surrounding matrix. In wood, a deformation model has been proposed for cell walls where the hemicellulose-lignin matrix transmit shear stresses between the stiff cellulose fibrils.[30] We have recently shown that shearing in the interfibrillar matrix is also a fundamental deformation mechanism in bone.[6] The helicoidal arrangement of fibrils in osteons is seen by the average angle μ over all cholesteric layers being different from zero (Fig. 3). This indicates that an osteon is designed for extensibility in tension, like a spring. We conclude that the deformation within osteons will occur mostly by shear between fibrils.

Our results show that osteons at the level of their microstructure are adapted to the *in vivo* mechanical stresses in bone. Since variations in self-assembly mechanisms and fibril orientation may occur, as a function of the local load at different locations in the tissue, a very promising avenue of research would be an investigation of possible biological

variance of the lamellar structure in an osteon. In general, however, the unidirectionality of the fibers around the blood vessel and the observed oscillation in fiber orientation in successive layers is a building block in understanding what biomechanical role the internal structure of the osteon phase plays, when embedded in the interstitial bone phase.

ACKNOWLEDGMENTS

[1] S. Weiner and H. Wagner, Annu. Rev. Mater. Sci. **28**, 271 (1998).

[2] M. M. Giraud-Guille, L. Besseau, and R. Martin, J. Biomech. **36**, 1571 (2003).

[3] J. Y. Rho, L. Kuhn-Spearing, and P. Zioupos, Med. Eng. Phys. **20**, 92 (1998).

[4] A. C. Neville, *Biology of fibrous composites: Development beyond the cell membrane* (Cambridge University Press, New York, NY, 1993).

[5] V. Ziv and S. Weiner, Connect. Tissue Res. **30**, 165 (1994).

[6] H. S. Gupta, W. Wagermaier, G. A. Zickler, D. Raz-Ben Aroush, S. S. Funari, P. Roschger, H. D. Wagner, and P. Fratzl, Nano Lett. **5**, 2108 (2005).

[7] J. D. Currey, *Bones: Structure and mechanics* (Princeton University Press, Princeton, N.J., 2002).

[8] M. Portigliatti Barbos, P. Bianco, A. Ascenzi, and A. Boyde, Metab. Bone Dis. Relat. Res. **5**, 309 (1984).

[9] T. G. Bromage, H. M. Goldman, S. C. McFarlin, J. Warshaw, A. Boyde, and C. M. Riggs, Anat. Rec. B New Anat. **274**, 157 (2003).

[10] A. Ascenzi, A. Benvenuti, A. Bigi, E. Foresti, M. H. J. Koch, F. Mango, A. Ripamonyi, and N. Roveri, Calcif. Tissue Int. **62**, 266 (1998).

[11] M. G. Ascenzi, A. Ascenzi, A. Benvenuti, M. Burghammer, S. Panza-volta, and A. Bigi, J. Struct. Biol. **141**, 22 (2003).

[12] D. Jaschouz, O. Paris, P. Roschger, H. S. Hwang, and P. Fratzl, J. Appl. Crystallogr. **36**, 494 (2003).

[13] H. R. Wenk and S. Grigull, J. Appl. Crystallogr. **36**, 1040 (2003).

[14] O. Paris, I. Zizak, H. Lichtenegger, P. Roschger, K. Klaushofer, and P. Fratzl, Cell Mol. Biol. (Paris) **46**, 993 (2000).

[15] P. Fratzl, M. Groschner, G. Vogl, H. Plenk, J. Eschberger, N. Fratzl-Zelman, K. Kolller, and K. Klaushofer, J. Bone Miner. Res. **7**, 329 (1992).

[16] I. Zizak, O. Paris, P. Roschger, S. Bernstorff, H. Amenitsch, K. Klaushofer, and P. Fratzl, J. Appl. Crystallogr. **33**, 820 (2000).

[17] C. Riekel and R. J. Davies, Curr. Opin. Colloid Interface Sci. **9**, 396 (2005).

[18] L. Calderin, M. J. Stott, and A. Rubio, Phys. Rev. B **67**, 134106 (2003).

[19] F. Heidelbach, C. Riekel, and H. R. Wenk, J. Appl. Crystallogr. **32**, 841 (1999).

[20] H. Wenk and F. Heidelbach, Bone (N.Y.) **24**, 361 (1999).

[21] W. J. Landis, K. J. Hodgens, J. Arena, M. J. Song, and B. F. McEwen, Microsc. Res. Tech. **33**, 192 (1996).

[22] S. Weiner, W. Traub, and H. D. Wagner, J. Struct. Biol. **126**, 241 (1999).

[23] A. P. Hammersley, S. O. Svensson, M. Hanfland, A. N. Fitch, and D. Hausermann, High Press. Res. **14**, 235 (1996).

[24] H. Lichtenegger, A. Reiterer, S. E. Stanzl-Tschegg, and P. Fratzl, J. Struct. Biol. **128**, 257 (1999).

[25] H. Lichtenegger, M. Müller, O. Paris, C. Riekel, and P. Fratzl, J. Appl. Crystallogr. **32**, 1127 (1999).

[26] P. Fratzl, Curr. Opin. Colloid Interface Sci. **8**, 32 (2003).

[27] A. Reiterer, H. Lichtenegger, S. Tschegg, and P. Fratzl, Philos. Mag. A **79**, 2173 (1999).

[28] M. M. Giraud-Guille, Curr. Opin. Solid State Mater. Sci. **3**, 221 (1998).

[29] S. C. Cowin, J. Non-Newtonian Fluid Mech. **119**, 155 (2004).

[30] P. Fratzl, I. Burgert, and H. S. Gupta, Phys. Chem. Chem. Phys. **6**, 5575 (2004).